

ADVANCED FUNCTIONAL MATERIALS

Supporting Information

for *Adv. Funct. Mater.*, DOI: 10.1002/adfm.201303547

Synthesis and Characterization of Gelatin-Based Magnetic Hydrogels

*Maria Helming, Baohu Wu, Tina Kollmann, Dominik Benke, Dietmar Schwahn, Vitaliy Pipich, Damien Faivre, Dirk Zahn, and Helmut Cölfen**

Supporting Information

Synthesis and Characterization of gelatin based magnetic hydrogels

By *Maria Helming*¹, *Baohu Wu*², *Tina Kollmann*³, *Dominik Benke*¹, *Dietmar Schwahn*⁴,

*Vitaliy Pipich*², *Damien Faivre*⁵, *Dirk Zahn*³ and *Helmut Cölfen*^{1,*}

XRD analysis

Figure S1 illustrates the X-ray diffraction (XRD) pattern of the magnetite/ gelatin composite and the iron loaded hydrogel. Both samples show a broad peak at 23 °C, which can be attributed to the amorphous nature of the biopolymer. The magnetite/ gelatin peak position and intensity coincide with crystallographic data for magnetite. However, this method is not appropriate to distinguish between the crystal structure of magnetite or maghemite, due to their similar diffraction pattern.

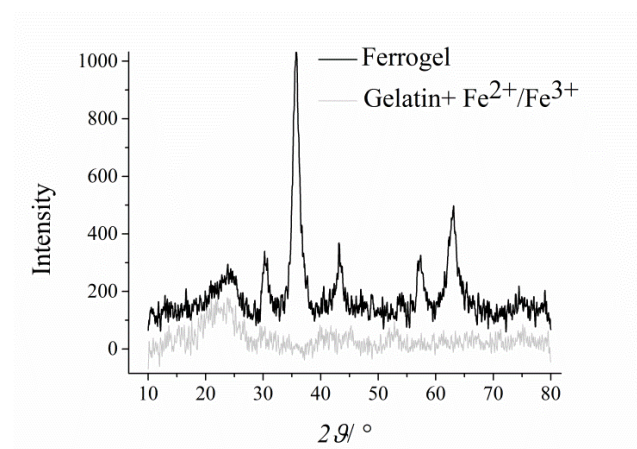


Figure S1. XRD pattern of representative ferrogel and gelatin samples loaded with iron (II) and iron (III) ions as reference.

TGA measurements

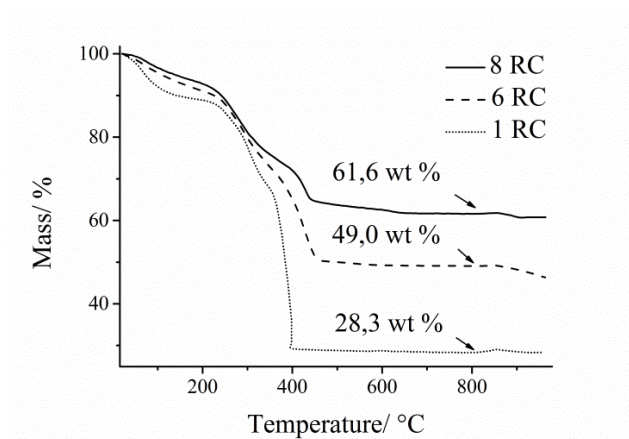


Figure S2. TGA curves of ferrogel consisting of 8 wt.-% gelatin in the wet state. RC stands for the number of reaction cycles.

SANS analysis

In this section we represent some more SANS data. Figure S3a shows the scattering from gels dissolved in D₂O of concentration Φ between 6 and 30 wt.-%. The scattering was normalized with gel volume fraction Φ . The so normalized scattering coincides at small Q , i.e. it shows same size of gel and a proportionality with respect to Φ . At large Q ($> Q_c$) one observes differences with respect to the mesh size, as compiled together with R_g of the gel in Table S1. A 12 wt.-% gelatin with and without magnetite is shown in Figure S3b. The contribution of magnetite becomes visible at large Q as already discussed in the main text.

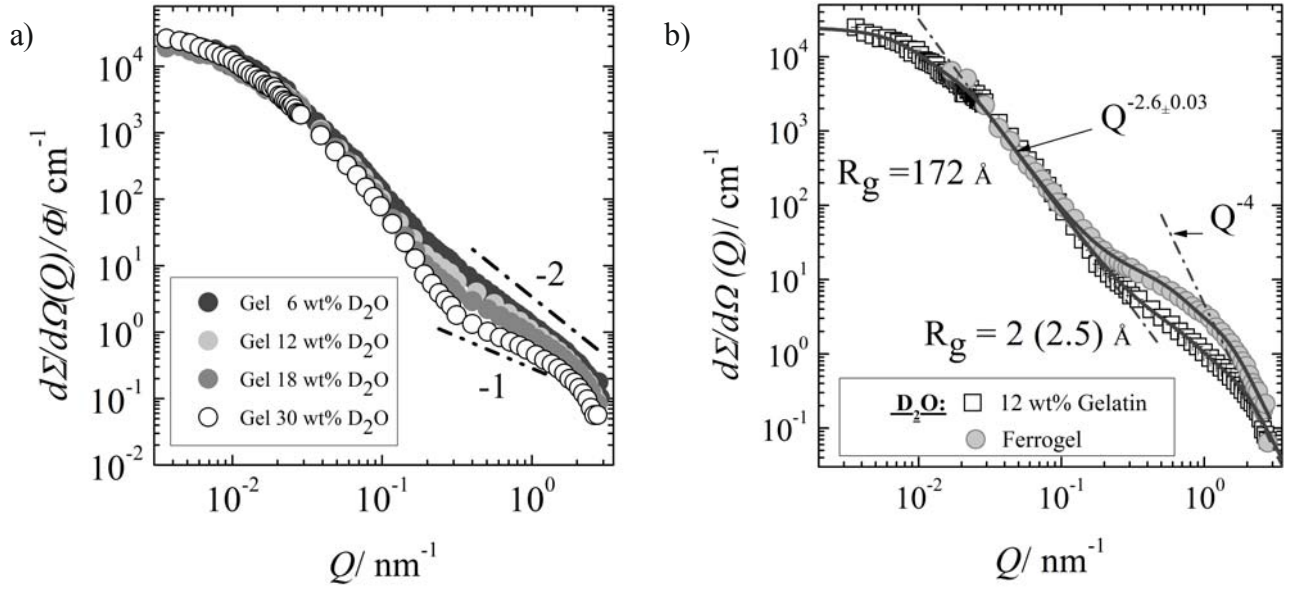


Figure S3. a) SANS macroscopic cross-section $d\Sigma/d\Omega$ versus scattering vector Q for gelatin in D_2O with concentrations from 6 to 30 wt.-%. The data are represented after rescaling with the gel volume fraction (Φ). b) Figure S4. SANS macroscopic cross-section $d\Sigma/d\Omega$ versus scattering vector Q for ferrogel in pure D_2O and pure gelatin 12 wt.-% in D_2O .

Table S1. The data extracted from Figure S3a.

	$R_{g,1}$ [nm]	$R_{g,2}$ [nm]	Q_c [nm^{-1}]	R_m [nm]
6 wt.-%	156	11.2	0.29	~ 22
12 wt.-%	155	15.9	0.28	~ 22
18 wt.-%	140	11.5	0.29	~ 22
30 wt.-%	191	11.7	0.31	~ 20

$R_{g,1}$ were extracted from $Q < 0.2 \text{ nm}^{-1}$, $R_{g,2}$ were extracted from $0.2 \text{ nm}^{-1} < Q < 1.5 \text{ nm}^{-1}$, R_m is the average mesh size estimated from $2\pi/Q_c$.

Structure factor analysis

The structure factor for the interpretation of scattering of the magnetite dispersed in ferrogel (Figure 5 and 6) is determined according to

$$S(Q) = 1 + \langle N \rangle \int_0^\infty dr 4\pi r^2 \{g(r) - 1\} \frac{\sin Qr}{Qr} \quad (S1)$$

with the averaged particle density $\langle N \rangle$, the particle density pair distribution function $g(r) = \exp[-\varepsilon(r)/k_B T]$ and $S(Q=0)=1$. The parameter $\varepsilon(r)$ represents the energy of interaction, r the distance between the particles, and k_B the Boltzmann constant. An ideal solution of spherical hard sphere particles is defined by the interaction potential and pair distribution function according to

$$\varepsilon(r) = \begin{cases} \infty & \text{for } r < 2R_s \\ 0 & \text{for } r > 2R_s \end{cases} \quad g(r)-1 = \begin{cases} -1 & \text{for } r < 2R_s \\ 0 & \text{for } r > 2R_s \end{cases} \quad (S2)$$

from which the analytic form of $S(Q)$ is evaluated as [Roe]

$$S(Q) = 1 - 8\Phi_s \frac{3(\sin 2QR_s - 2QR_s \cos 2QR_s)}{(2QR_s)^3} \quad (S3)$$

The parameter Φ_s represents the volume fraction of fictitious "hard sphere" particles of radius R_s , describing the range of excluded volume interaction according to eq S2. In case of $\Phi_s \rightarrow 0$ $S(Q)$ becomes 1 and the scattering is determined solely by the form factor of the magnetite particles.

Table S2. SAXS parameters obtained from fit of the structure factor $S(Q)$ in combination with "Beaucage" equation.

	18 wt.-% Ferrogel		12 wt.-% Ferrogel	
	Wet	Dry	wet	Dry
$d\Sigma/d\Omega(0)$ [cm^{-1}]	28±0.11	456±20	32.6±0.2	178±6
R_g [nm]	10±0.1	10 (!)*)	8.7±0.1	8.7 (!)*)
P_a [$\text{cm}^{-1} \text{nm}^{-a}$]	$P_{2.73} = 0.33 \pm 0.004$	$P_3 = 1 \pm 0.01$ $Q > 2.3 \text{ nm}^{-1}$: $P_4 = 7.3$	$P_3 = 0.511 \pm 0.002$	$P_3 = 2.63 \pm 0.01$ $Q > 2.3 \text{ nm}^{-1}$: $P_4 = 5.3$
Φ_s [10^{-2}]	7.2±0.04	12.4±0.1	8.5±0.05	11.6±0.1
R_s [nm]	11.2±0.1	3.7±0.02	10.2±0.14	3.75 ±0.03

*)) We assumed that R_g of the form factor is the same for "wet" and "dry" samples.

Table S3. SANS parameters of 18 wt.-% ferrogel in wet condition from Figure 5.

$d\Sigma/d\Omega(0)$ [cm^{-1}]	R_g [nm]	P_2 [$10^{-1} \text{ cm}^{-1} \text{ nm}^{-2}$]	Φ_S [10^{-2}]	R_S [nm]	P_4 [$\text{cm}^{-1} \text{ nm}^{-4}$] ($Q > 1.43 \text{ nm}^{-1}$)
8.3±3.6	10.4±1.2	0.106±0.008	7.6±2.2	7±2.6	0.19